JOURNAL OF MATERIALS SCIENCE **35** (2000) 1911–1916

The role of fluorine in the devitrification of $SiO_2{\cdot}Al_2O_3{\cdot}P_2O_5{\cdot}CaO{\cdot}CaF_2$ glasses

KEN STANTON, ROBERT HILL*
Department of Materials Science and Technology, University of Limerick, Ireland
E-mail: r.hill@ic.ac.uk

A series of eight glasses based on a glass system with the generic composition $1.5(5-Z)SiO_2{\cdot}(5-Z)\ Al_2O_3{\cdot}1.5P_2O_5{\cdot}(5-Z)CaO{\cdot}ZCaF_2$ were studied where $Z = 2$, 1.75, 1.5, 1.25, 1, 0.5, 0.25, 0. These glasses were characterised using differential scanning calorimetry (DSC) and x-ray powder diffraction (XRD). Glasses with high fluorine contents were found to crystallise readily to fluorapatite via a homogeneous nucleation route probably involving prior amorphous phase separation. These results are explained in terms of an approach which views glasses as being inorganic polymers where the presence of fluorine disrupts the glass network and thereby reduces the energy barrier to homogeneous nucleation and crystallisation of fluorapatite.

1. Introduction

A variety of glass-ceramics have been developed during the last 25 years for biomedical and dental applications. These materials generally fall into one of three general categories. Firstly there are the apatite-wollastonite ceramics developed by Kokubo *et al.* [1] based on a $SiO_2{\cdot}P_2O_5{\cdot}CaO{\cdot}MgO$ system. Then there are the mica-based materials that were originally developed by Beall *et al.* [2] and Grossman [3]. The latter class of material includes Dicor™ which is commercially available and is used for producing dental crowns [4]. Finally, then, there are apatite-mullite glass-ceramics [5–7].

Both the apatite-wollastonite and apatite-mullite systems contain an apatite as a primary crystalline phase—in the case of the latter system, fluorapatite is the specific phase formed. It is desirable to use an apatite containing material for biomedical applications because apatite is the crystalline phase that naturally constitutes the major proportion of human tooth and bone.

Apatite-mullite glass-ceramics are the subject of the present discussion. These materials have been developed largely as a result of research into improved glasses for incorporation into glass-ionomer cements—a type of dental restorative material [8–11]. Glasses for this application generally contain 20–36 wt.% SiO_2, 15–40% Al_20_3, 0–35% CaO, 0–10% $AlPO_4$, 0–40% CaF_2, 0–5% Na_3AlF_6 and 0–6% AlF_3. Glasses of this nature may be generally referred to as *ionomer glasses*. These were originally developed empirically from the dental silicate glasses invented around the turn of the century. Recent development of these glasses, however, has been more systematic [12–14] and has led to the development of new glass compositions that do not lose significant amounts of silicon tetrafluoride during melting—a serious deficiency of earlier systems.

For further development of these glasses, we must endeavour to obtain a detailed understanding of role of the individual structural components of the glass and how they interact within the glass. In this way we may optimise the glass and glass-ceramic processing regimes to give a glass with the desired properties (e.g. castability, translucency, fracture toughness etc.).

One of the components of biomedical glasses and glass-ceramics that is essential to understand is fluorite. The reasons for this are manifold and various. King *et al.* [15] have noted that for glass-ionomer cement systems, the incorporation of fluorine increases the working time of the cement by delaying the bonding of metal cations such as Al^{3+} and Ca^{2+} to the polyacid chains by the formation of intermediate fluoride complexes. It has also been noted that fluoride ions present in human saliva and blood plasma are essential for normal development of hard tissue development in the body [16].

With regard to the apatite-mullite materials considered in the present study, an understanding of the role of fluorine is important because of the potential of these materials to be cast to shape. Increasing amounts of fluorine, as will be shown, reduces the glass transition temperature, T_g, and the melt temperature, T_m, of a glass. Fluorine content also has major implications for the crystallisation of a glass to a glass-ceramic both in terms of the crystallisation mechanism and the phases formed.

In order to carry out work of this nature a meaningful model is needed. There are today several theoretical approaches which one may use to make predictions about the behaviour of a glass in terms of its constituents. These generally stem from either the Zachariasen random network theory [17] or Lebedev's

* Author to whom all correspondence should be addressed.

crystallite theory [18]. A further useful approach is that taken by Holliday [19] which views inorganic glasses as being *inorganic polymers*. It is obvious that there are certain similarities between organic and inorganic polymers such as the fact that both classes of materials exhibit glass transition temperatures and high melt viscosities.

Inorganic silicate glasses, then, may be considered to be polymers of oxygen crosslinked by silicon atoms. The polymer chains in an inorganic glass may be considered to be cross-linked to a greater or lesser degree depending on whether one sees the inherent structure of glass as being a random network or composed of crystallites with some localised medium-range order. The degree of crosslinking may be considered to be a function of the scale at which one considers the structure of glass. However, both random network and crystallite approaches will have the same number of crosslinks per unit length of the chain when averaged over a long range.

It is possible to adopt a classification system based on the network connectivity [20] which is defined as the average number of bonds that link each repeat unit in the network. This idea may then be developed to define the *crosslink density* of the glass which is the average number of additional crosslinking bonds above two for the elements other than oxygen forming the glass network. Thus, a glass with a network connectivity of 2, equivalent to a crosslink density of 0, corresponds to a linear polymer chain while a pure silica glass has a network connectivity of 4 and a crosslink density of 2. The network connectivity and crosslink density of a glass can be used to make predictions about such glass properties as surface reactivity, expansion coefficient, solubility and likelihood of undergoing amorphous phase separation or glass-in-glass phase separation and has been used in the past to explain the reactivity and bioactivity of bioglasses [21]. Using this approach also allows us to make certain predictions about the behaviour of glass using ideas from polymer science. For example it is possible to model the glass transition temperatures of many inorganic glasses using the Gibbs–Di Marzio equation [22].

The inorganic polymer approach to glass structure, then, constitutes a useful qualitative context within which to work when considering the effects of various additions to an glass.

2. Materials and methods

2.1. Glass synthesis

The glass components silica (SiO_2), alumina (Al_2O_3), phosphorus pentoxide (P_2O_5), calcium carbonate ($CaCO_3$) and calcium fluoride (CaF_2) were weighed into the appropriate molar ratios for the production of six glasses with the generic composition

$$1.5(5-Z)SiO_2 \cdot (5-Z)Al_2O_3 \cdot 1.5P_2O_5 \cdot (5-Z)CaO \cdot ZCaF_2$$

where $Z = 2$, 1.75, 1.5, 1.25, 1, 0.5, 0.25, 0. It may be seen that this formula ensures a fixed ratio of $CaO : Al_2O_3 : SiO_2$ of 2 : 2 : 3 and a fixed ratio of Ca : P of 5 : 3. This latter ratio is the ratio of calcium to phosphate in the apatite crystalline phase ($Ca_5(PO_4)_3F$). There is also sufficient Ca^{2+} ions to charge balance the Al^{3+} ions in the glass structure and maintain them in a tetrahedral four fold coordination state.

TABLE I Z-values, firing times, firing temperatures and calculated crosslink density values for each of the eight glasses. Crosslink density values were calculated according to Ray [20]

Glass	Z-value	Firing temp /°C	Crosslink density value
LG26	2	1420	1.19
LG246	1.75	1420	1.26
LG180	1.5	1430	1.33
LG247	1.25	1430	1.41
LG27	1	1430	1.59
LG28	0.5	1495	1.73
LG29	0.25	1450	1.8
LG30	0	1535	1.85

Batches of approximately 500 g were produced at a time. The powdered components were mixed in a ball mill before being transferred to a mullite crucible. The crucible and charge were then heated in an electric furnace at temperatures of between 1350 and 1500 °C for two hours. The glass melt was then shock quenched by pouring directly into demineralised water to produce glass frit. This material was then dried in a vacuum oven for 1 day before being ground in a vibratory mill. The glasses were then sieved to produce powders with particle sizes of <45 μm, >45 μm to <125 μm and >125 μm. These particle sizes will henceforth be referred to as <45 μm, coarse and frit respectively. Firing temperatures are shown in Table I for each glass along with codes allocated to each glass.

2.2. Differential scanning calorimetry

Differential scanning calorimetry (DSC) was used to identify the nucleation mechanisms of the glasses. The instrument used was a Stanton-Redcroft DSC 1500 capable of analysing samples up to 1500 °C. Samples of 50 mg were contained in platinum crucibles and heating rates of 10 °C/min were used throughout. Two analytical regimes were used. The first type of analysis was a simple comparison of the traces yielded by samples of frit, coarse and <45 μm particle sizes of glass. This type of analysis is useful in determining whether a glass will crystallise via a surface (or *heterogeneous*) nucleation route. The rationale behind how this analysis works is that on moving to smaller particle sizes, the amount of surface area per unit volume of glass will increase. This offers a greater chance that surface nucleation will occur if the glass is prone to surface nucleation. If the glass under examination does indeed nucleate and crystallise via a surface route then a pronounced sharpening of crystallisation peaks will occur with decreasing particle size. A further effect is that crystallisation peaks move to a lower temperature with decreasing particle size.

The second analytical regime that was used was devised by Marotta *et al.* [23]. This technique facilitates the determination of the optimum nucleation

temperature (in other words, the temperature at which the nucleation rate is at a maximum) of glasses using DSC. This technique may be applied to all glass systems that undergo internal crystal nucleation and has several advantages including the fact that all heat treatment is carried out inside the DSC furnace so that only the DSC equipment needs to be used. Also, only a small amount of material is needed (<300 mg).

Marotta *et al.* postulated that the number of stable nuclei N_n formed in a sample per time element t_n is

$$N_n = I t_n^b \quad (1)$$

where I is the kinetic rate constant of nucleation and b is a parameter related to the nucleation mechanism. Marrotta also showed that if t_n is the same for each sample at each temperature T_n then the following expression applies:

$$\ln I = \frac{E_c}{R}\left[\frac{1}{T_{p'}} - \frac{1}{T_p}\right] + \text{constant} \quad (2)$$

where E_c is the activation energy for crystallisation, R is the gas constant, $T_{p'}$ is the temperature at which a crystallisation peak occurs after a nucleation hold and T_p is the temperature at which the latter crystallisation peak occurs at without a nucleation hold.

The method is employed practically by heating a sample to its glass transition temperature, T_g, and holding it there for an hour. The sample is then heated beyond its melting temperature. More samples are then subjected to the same regime but with the hold temperature increasing by some increment, say 15 °C, each time. $T_{p'} - T_p$ is then plotted against T_n. A nucleation rate against temperature curve is then obtained.* The maximum of this curve is, of course, the optimum nucleation temperature for the glass.

Heating rates of 10 °C/min were used for the determination of all optimum nucleation curves and typically, five runs were carried out for each material; i.e. with nucleation holds at T_g and $T_g + 15$, 30, 45, 60 °C. This regime did vary, however, if it was felt that it was necessary to look at a certain glass over a given temperature range.

Coarse material was used for all optimum nucleation studies. If <45 μm material had been used then the surface area per unit volume of material would have been greater and surface nucleation effects (if present) would have overwhelmed the effects of any bulk nucleation that may have been happening simultaneously. Conversely, frit is not used because there is not enough surface area for surface nucleation effects to become obvious. Also, it is relatively difficult to get very reproducible results using frit because of the nature of the material; DSC runs of frit only use between 2 and 10 particles (together weighing 50 mg) and variations in the way these particles contact the crucible and/or settle during the run may produce slight variations in the results.

* It may be seen that according to Equation 2, Marrotta advocates the plotting of $(1/T_{p'}) - (1/T_p)$ against T_n. However, the present method was used because it is felt that this gives a more accurate picture of nucleation events: Marrotta's method may show even relatively minor fluctuations as noticeable features.

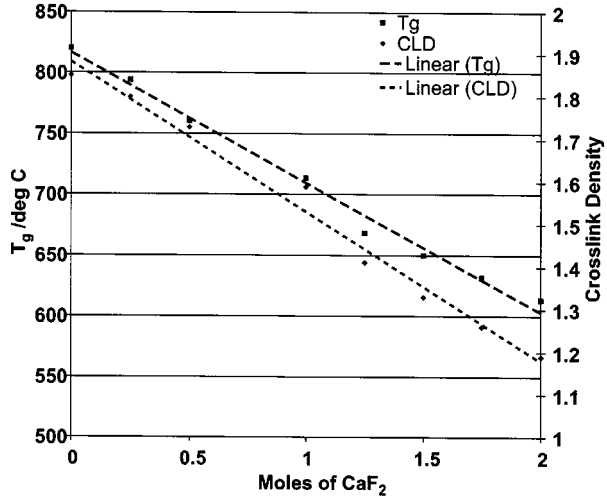

Figure 1 Plot of inverse relationship between T_g and crosslink density with increasing fluorine content.

2.3. X-ray powder diffraction analysis

All X-ray powder diffraction (XRD) analysis of the samples was carried out in a Phillips Expert powder X-ray diffractometer† using Cu-K_α radiation between 10 and 70 °2θ. The scan time over this angular range was 25 mins.

All heat treatment of samples for X-ray diffraction was carried out in a dental porcelain furnace. Samples were heated at a rate of 10 °C/min to mimic the conditions of the DSC experiments and were quenched to room temperature immediately upon reaching the target temperature.

3. Results

The glass transition temperature T_g was noted for each glass at 10 °C/min. T_g values are given in Table III and are plotted against fluorine content for each glass in Fig. 1. Also plotted in Fig. 1 are the calculated crosslink density (CLD) values. It can be seen that there is a very close linear relationship between the fluorine content and the T_g and CLD values. Therefore we can say that there is also a very close linear relationship between T_g and CLD.

The results from DSC analysis of three different particle sizes of the six glasses are shown in Table II. It will be seen that the T_{p_2} crystallisation peak for <45 μm LG180 splits. It is thought that this is likely due to a slight change in the composition due to loss of fluorine as a result of the volatilisation of silicon tetrafluoride. It is also more likely to happen in <45 μm material because of the large surface area to volume ratio.

It may be seen that T_{p_1}, moves to a lower temperature with decreasing particle size for every glass except for LG26 and LG246—the glasses with the highest fluorine

† Phillips, Eindhoven, NL.

TABLE II Results from DSC analysis of three different particle sizes showing the positions of the first and second crystallisation peaks; T_{p_1} and T_{p_2} respectively. Where two values are shown, the peak has split slightly. Where no value is given, there was no observed peak

		<45 μm		Coarse		Frit	
Glass	Z-value	T_{p_1}	T_{p_2}	T_{p_1}	T_{p_2}	T_{p_1}	T_{p_2}
LG26	2	740	930	739	946	739	931
LG246	1.75	778	977	776	1000	775	994
LG180	1.5	855	990/1040	858	1032	855	1057
LG247	1.25	875	991	—	1015	1008	1087
LG27	1	977	—	994	—	1043	1107
LG28	0.5	1056	—	1071	—	1129	—
LG29	0.25	1045	—	1086	—	1183	—
LG30	0	919	1097	930	1053	961	1186

TABLE III Results from optimum nucleation temperature analysis of glasses using DSC with coarse particle size powders. All values are in °C. No values are given for LG247 because $T_{p_1'}$ was very broad and indistinct for all of the holds

Glass	Hold temp.	T_p	$T_{p'} - T_p$
LG26	640	725	14
$Z = 2.0$	650	721	18
($T_g = 613$)	660	720	19
($T_{p'} = 739$)	670	716	22
LG246	648	764	13
$Z = 1.75$	663	745	32
($T_g = 632$)	686	711	36
($T_{p'} = 777$)	705	760	17
LG180	615	863	−4
$Z = 1.5$	632	850	9
($T_g = 650$)	653	823	36
($T_{p'} = 859$)	673	800	59
	691	805	54
	712	833	26
	730	847	12
LG27	714	993	1
$Z = 1.0$	729	1003	−9
($T_g = 714$)	744	999	−5
($T_{p'} = 994$)	759	998	−4
	774	1000	−4
LG28	761	1094	−23
$Z = 0.5$	776	1085	−14
($T_g = 761$)	791	1087	−16
($T_{p'} = 1071$)	806	1085	−14
	821	1089	−18
LG29	794	1090	−4
$Z = 0.25$	809	1089	−3
($T_g = 794$)	824	1087	−1
($T_{p'} = 1086$)	839	1091	−5
	854	1096	−10
LG30	820	1108	−55
$Z = 0$	835	1105	−52
($T_g = 820$)	850	1111	−58
($T_{p'} = 1053$)	865	1101	−48
	880	1107	−54

content. This would indicate that every glass except for LG26 and LG246 has surface nucleation characteristics with respect to the position of T_{p_1}. The behaviour characterised by a surface nucleation process is illustrated for LG27 in Fig. 2.

All results from the optimum nucleation study are presented in Table III. In each case T_p corresponds to the first crystallisation peak or T_{p_1}. T_g values are for onset of the glass transition. T_p is the temperature at which the dominant crystallisation peak occurred with a hold for one hour at T_n and $T_{p'}$ is the temperature at which the same crystallisation peak occurred in a straight run; i.e. without a nucleation hold.

It will be seen that only LG26 ($Z = 2$), LG246 ($Z = 1.75$) and LG180 ($Z = 1.5$) exhibit optimum nucleation curves and therefore optimum nucleation temperatures. All other glasses show no significant variation in $T_{p'} - T_p$ over the various holds in temperature. This means that only LG26 and LG180 will bulk nucleate when subjected to a 1 hour hold. A typical optimum nucleation curve—the curve for LG180—is given in Fig. 3.

XRD results are given in Table IV.

TABLE IV Principal crystalline phases observed in each glass using XRD

Glass	Z-value	Observed phases at T_{p_2}
LG26	2.0	Fluorapatite and mullite
LG246	1.75	Fluorapatite and mullite
LG180	1.5	Fluorapatite and mullite
LG247	1.25	Fluorapatite and mullite
LG27	1.0	Fluorapatite and mullite
LG28	0.5	Fluorapatite, mullite and anorthite (small amount)
LG29	0.25	Fluorapatite, mullite and anorthite (large amount)
LG30	0	Anorthite

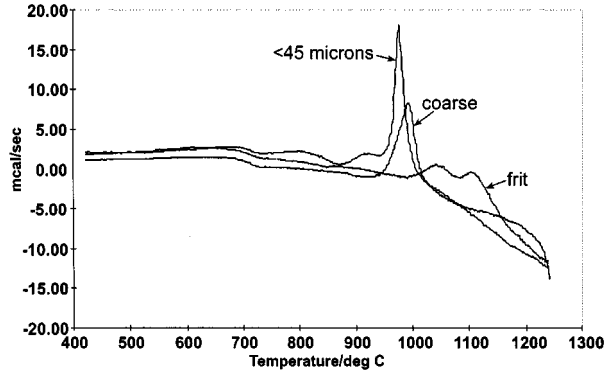

Figure 2 DSC traces for three particle size analysis of LG27 ($Z = 1.0$).

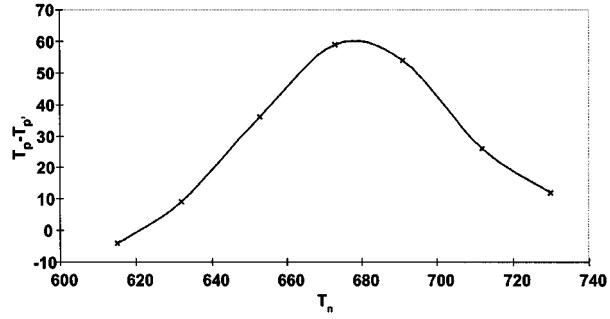

Figure 3 Optimum nucleation curve for glass LG180 ($Z = 1.5$).

4. Discussion

The first validation for using crosslink density as a guide to how a glass will behave is given by the T_g data given in Table III and plotted in Fig. 1. As previously

noted, there is a very close linear relationship between calculated crosslink density values and T_g values for each glass. So while crosslink density is really nothing more than a mathematical construct arising from some relatively simple assumptions, it does seem to work relatively well as a general qualitative tool.

Of the work presented, perhaps the most interesting results are those for the glass LG180 when examined in the context of its behaviour relative to the results given by LG26 and LG27. LG246 and LG247 are intermediary in both composition and behaviour relative to these glasses.

It may be seen that LG180 has surface nucleation characteristics (as determined by DSC analysis of three different particle sizes) but it will also bulk nucleate when subjected to an isothermal hold at some temperature above it's glass transition temperature. The optimum hold temperature to cause nucleation of the glass is 678 °C, i.e. $T_g + 28$ °C. This means that LG180, having a composition that is intermediate between LG26 and LG27, also has nucleation characteristics that are intermediate between the respective bulk and surface nucleating characteristics of LG26 and LG27.

It has previously been postulated [24] that the most important factors that determine whether a glass will bulk nucleate to fluorapatite are as follows:

1. That the Ca : P ratio be 5 : 3 which is the Ca : P ratio in the apatite phase.
2. That there be sufficient fluorine present from a chemical/compositional point of view for the fluorapatite phase to form.

The results presented in the present work, however, would indicate that while these points are probably very important, they most certainly are not the sole deciding factors. It is now apparent that small compositional variations in the amount of fluorine present can dramatically affect the likelihood of the bulk nucleation of fluorapatite. LG27 is not fluorine deficient with respect to the fluorapatite stoichiometry yet it will not bulk nucleate when subjected to one hour isothermal holds. LG180, however, with its lower crosslink density will do so quite readily showing a classic optimum nucleation curve and a distinct optimum nucleation temperature.

This is easily explained in terms of our inorganic polymer model. As we reduce the amount of fluorine present, we increase the crosslink density and this hinders amorphous phase separation and forms an energy barrier to bulk nucleation. Because surface nucleation will typically occur under conditions of lower energy, then this is what occurs when the energy barrier to bulk nucleation is too great. In the case of LG180, this is what occurs. Under conditions of being steadily ramped up in temperature, the glass does not have enough energy available to it to overcome the energy barrier to bulk nucleation caused by the relatively high crosslink density of the glass. However, when the glass is held for an hour at a suitable temperature below the crystallisation temperature, then it gains enough energy to overcome this barrier.

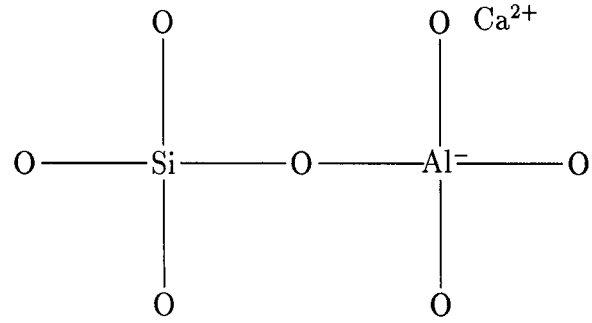

Figure 4 Charge compensation by calcium. Al^{3+} is short of one unit of positive charge to take up a four coordinate role in the glass network. Two Al^{-} ions can be charge compensated by an adjacent Ca^{2+} ion.

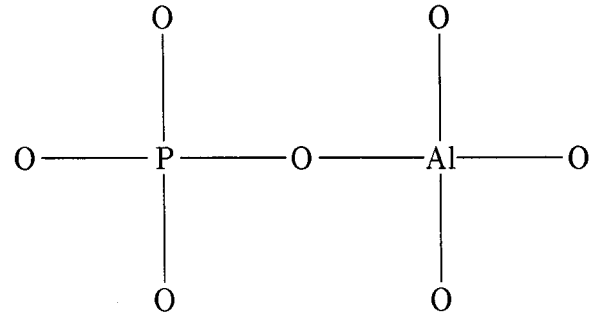

Figure 5 Charge compensation by phosphorus: Al^{3+} is short of one unit of positive charge to take up a four coordinate role in the glass network. Al^{3+} in a four-fold coordinate state can be charge compensated by an adjacent P^{5+}. $AlPO_7$ is structurally similar to Si_2O_7.

Fluorapatite (FAP) was the first to be detected by XRD. The relative amount of FAP reduced as Z, the amount of CaF_2 added to the glass melt was reduced. In the glasses with the two highest Z values T_{p_1} corresponded to FAP and T_{p_2} to mullite. Increasing amounts of anorthite were formed as Z decreased.

Evidence in the literature would suggest that the high fluorine glasses ($Z > 1.0$) undergo phase separate to a calcium phosphate rich glass phase and an aluminosilicate rich glass phase and these subsequently crystallise to FAP and mullite [6, 25].

Mullite crystallisation is surprising at first at such low temperatures. However, crystallisation of FAP will remove calcium and phosphate ions from the glass network that are required to charge balance Al^{3+} and maintain them in a four-fold coordination. This is shown schematically in Figs 4 and 5. Removal of phosphate and calcium will force Al^{3+} ions into a higher coordinate state by removal of the charge balancing cations and in the case of P^{5+} will force AlO_4 into close proximity which again will force the Al^{3+} ion into higher coordinate states and force mullite crystallisation in which aluminium is in a mixture or 4 and 6 coordinate states [26].

The reduced amount of FAP that forms as a result of reducing the fluorine content will leave more calcium and phosphate in the glass to charge balance the Al^{3+}. In these circumstances crystallisation of anorthite is favoured in which calcium charge balances Al^{3+} ions in a four-fold coordination state [24].

5. Conclusions

The exact amount of fluorine in an ionomer glass composition may have a dramatic effect on the nucleation and crystallisation behaviour of the glass. This effect is not only a result of the stoichiometric considerations of crystal formation but also of the network disrupting role of fluorine within a glass network.

In order to design a glass with optimum properties for future dental or biomedical applications the amount of fluorine needs to be carefully controlled. This is especially true from a microstrctural perspective.

Acknowledgements

The authors would like to gratefully acknowledge the support of Brite EuRam Contract BRPR-CT96-0320.

References

1. T. KOKUBO, M. SHIGEMATSU, Y. NAGASHIMA, T. TASHIRO, T. NAKURA and H. HIGASHI, *Bull. Inst. Chem. Red Kyoto Univ.* **30** (1982) 260.
2. G. J. H. BEALL, M. R. MONTIERTH and P. SMITH, *Barbeithare Glaskeramik Umshance* **42** (1972) 468.
3. US Patent no. 3839055 (1974).
4. P. J. ADAIR and D. G. GROSSMAN, *Int. J. Periodent. Res. Dent.* **2** (1984) 683.
5. R. G. HILL, M. PATEL and D. J. WOOD, in "Bioceramics" Vol. 4, edited by W. Bonfield, G. W. Hastings and K. E. Tanner (Butterworth-Heinemann, London, 1991).
6. R. HILL and D. WOOD, *J. Mat. Sci.: Materials in Medicine* **6** (1995) 311.
7. A. CLIFFORD and R. HILL, *J. Non-Crys. Solids* **196** (1996) 346.
8. A. D. WILSON and H. J. PROSSER, *Br. Dent. J.* **157** (1984) 449.
9. S. CRISP and A. D. WILSON, *J. Dent. Res.* **53** (1974) 1408.
10. *Idem., ibid.* **53** (1974) 1414.
11. *Idem., ibid.* **53** (1974) 1420.
12. D. WOOD and R. G. HILL, *Biomaterials* **12** (1991) 164.
13. R. G. HILL, C. GOAT and D. WOOD, *J. Amer. Ceram. Soc.* **75** (1992) 778.
14. A. S. RIZKALLA, D. W. JONES, E. J. SUTOW and G. C. HALL, *J. Dent. Res.* **70** (1991) 461.
15. H. W. KING, E. A. PAYZANT, D. W. JONES and A. S. RIZKALLA, *Journal of the Canadian Ceramic Society* **62** (1993) 248.
16. L. J. JHA, S. M. BEST, J. C. KNOWLES, I. REHMAN and J. D. SANTOS, *J. Mat. Sci.: Materials in Medicine* **8** (1997) 185.
17. W. J. ZACHARIASEN, *J. Amer. Ceram. Soc.* **54** (1932) 3841.
18. A. A. LEBEDEV, *Trudy Cossud Opt. Inst.* **2** (1921) 57.
19. L. HOLLIDAY, *Inorg. Macromol. Rev.* **1** (1970) 3.
20. N. H. RAY, "Inorganic Polymers" (Academic Press, London, 1978).
21. R. HILL, *J. Mat. Sci. Letters* **15** (1996) 1122.
22. L. A. DI MARZIO and J. H. GIBBS, *Polym. Sci.* **40** (1959) 121.
23. A. MAROTTA, A. BURI, F. BRANDA and S. SAIELLO, in "Advances in Ceramics" Vol. 4, edited by J. H. Simmons, D. R. Uhlmann and G. H. Beall (The American Ceramic Society, 1982)
24. ANTON CLIFFORD, PhD thesis, University of Limerick, 1997.
25. C. JANA and W. HOELAND, *Silicates Industriels* **56** (1991) 215.
26. W. LOWENSTEIN, *Am. Mineral* **39** (1954).

Received 19 February
and accepted 28 September 1999